



室蘭工業大学

学術資源アーカイブ

Muroran Institute of Technology Academic Resources Archive



Oxidation of CuSn alloy nanotree and application for gas sensors

メタデータ	言語: English 出版者: The Japan Society of Applied Physics 公開日: 2017-03-28 キーワード (Ja): キーワード (En): 作成者: 金子, 直人, 清水, 智弘, 多田, 芳広, 新宮原, 正三 メールアドレス: 所属:
URL	http://hdl.handle.net/10258/00009184

Oxidation of CuSn alloy nanotree and application for gas sensors

Naoto Kaneko¹, Tomohiro Shimizu¹, Yoshihiro Tada², and Shoso Shingubara¹

**¹ Graduate School of Science and Engineering, Kansai University, Suita, Osaka
564-8680, Japan**

² Muroran Institute of Technology, Muroran, Hokkaido 050-0071, Japan

The CuSn alloy nanotree formed by DC electroplating is a true three-dimensional (3D) structure with many branches that separate the trunk perpendicularly. We carried out the oxidation of CuSn nanotrees in atmosphere in order to study the possibility of such nanotrees for application to sensors. It was confirmed that the oxygen concentration in the CuSn nanotree oxide increased with temperature and reached 40 at.% at 350 °C. The optical reflectance spectra of the CuSn nanotree oxide formed at 250 °C showed a 3 - 4% reflectance in the wavelength range between 400 and 900 nm, and its behavior differed from those of Cu and Sn oxides formed at 250 °C. The temperature dependence of electrical resistivity for the CuSn nanotree oxide showed a typical semiconductor behavior. By the introduction of H₂, O₂, N₂, and CO gases into the chamber, the resistance of the CuSn nanotree oxide responded against H₂ most sensitively, as well as against O₂ and CO gases. From the resistance change tendency, it is strongly suggested that the CuSn nanotree oxide is a p-type semiconductor, because it shows an increase in conductivity caused by the adsorption of a negative charge such as O⁻. However, the conductivity decreases with the adsorption of a positive charge such as H⁺. The present study suggests the high potential of the CuSn nanotree oxide as a gas sensor, since it has a very high surface-to-volume ratio.

1. Introduction

A nanotree is a true three-dimensional (3D) structure with many branches that separate the trunk perpendicularly, and sub-branches grow perpendicularly from them also, as shown by DC electroplating with a constant potential mode. The branch diameter distributes between 30 – 200 nm, so it is called a CuSn nanotree [1].

Recently, oxide semiconductor gas sensors with a 3D structure have been studied. As semiconductor materials, for example, WO_3 [2,3], ZnO [4-6], TiO_2 [5], CuO [3,5], and SnO_2 [6,7] are used. Among them, SnO_2 is most widely used as a gas sensor and the detection target is a reducing gas such as H_2S [8-11]. Additionally, it is important for sensor materials to have a high surface-to-volume ratio because the gas sensing mechanism is based on the conductivity change occurring at the surface [6].

There have been low-dimensional structures with a high surface-to-volume ratio, including 1D structures such as nanowires [12-15], nanorods [16,17], nanocones [18], nanoparticles [19,20], and whiskers [21,22], and 2D structures such as nanodisks [23], and nanoplates. Furthermore, 3D nanostructures such as nanotrees [5,24], nanoforests [25,26], nanoflowers [7,27], and pine tree nanowires [28,29] are expected to exhibit excellent properties as sensors [30]. However, there have been few studies describing the formation of 3D nanostructures of CuSn alloy by self-organization. A CuSn nanotree is a true 3D structure with many nanosized branches and therefore it has a very high surface-to-volume ratio. The oxide of CuSn nanotrees is expected to have excellent properties as a gas sensor material.

In this work, we studied the formation of a CuSn nanotree oxide by annealing CuSn

nanotrees in atmosphere, particularly aiming at the formation of semiconducting nanotrees. Then, we evaluated the optical and electrical conduction properties of this material in order to examine the possibility of such a material for application to sensors. We evaluated the optical properties by reflectance spectra measurement, and also measured resistance change properties when reactive gases were introduced.

2. Sample preparation

CuSn alloys were electrodeposited on 200-nm-thick sputtered Pt films on Si substrates. Prior to electrodeposition, the Pt surface was cleaned with isopropanol and deionized water in an ultrasonic bath. CuSn nanotrees were prepared using a CuSn alloy plating bath containing copper nitrate, tin chloride, oxalic acid, and poly(ethylene glycol) (PEG1000) with DC electrodeposition in a constant potential mode. Ag|AgCl and platinum electrodes were used as reference and counter electrodes in the electrochemical cell, respectively. The Pt-coated Si substrate on a rotating disc electrode was used as the working electrode, which is the cathode. The rotation speed of the disc was maintained at 50 rpm. The CuSn plating bath temperature was 55 °C and pH was 3.5. A plating potential of -0.6 V was applied to the working electrode during the formation of CuSn nanotrees.

The morphology of the electrodeposited CuSn alloy was observed by scanning electron microscopy (SEM; JEOL JEM-7500F), and the crystalline structure and atomic ratio of deposits were analyzed by transmission electron microscopy (TEM; JEOL JEM-2100F) with an energy-dispersive X-ray analysis (EDX) measurement system.

The oxidation of CuSn nanotrees was carried out in air atmosphere at temperatures between 100 and 400 °C, and reflectance spectra were measured. Furthermore, the change in the electrical resistance of the CuSn nanotree oxide was measured concomitantly with

the introduction of reactive gases into the chamber.

3. Results and discussion

Figure 1 shows cross-sectional SEM images of the electrodeposited CuSn alloy on the Pt electrode by dc electrodeposition at a constant potential. It is remarkable that nanotrees with many perpendicular branches were formed at -0.60 V for the working electrode. Each branch has a one-dimensional structure with a diameter of around a few tens of nm, and grows perpendicularly from the branch. At the top view of a nanotree, fourfold symmetrical branches grown perpendicular to the trunk of the tree were observed as shown in Fig. 1(b).

A nanotree structure with many branches was formed by electroplating for more than 1 h. The height and number of branches of this nanotree increased with increasing electrodeposition time. The structure of the branches is perfectly organized, and the diameter of each branch is a few tens of nm [Figs. 1(c) and 1(d)]. Each nanotree branch is a single crystal, because there is no grain boundary, and we observed a regular array of atoms by lattice imaging. In addition, it was revealed that each nanowire of the nanotrees consists of gamma-phase cubic Cu₃Sn, and the growth directions of the branches are $\langle 100 \rangle$ and $\langle 110 \rangle$. The lattice spacing measured by diffraction spots agrees well with the literature values of gamma-phase Cu₃Sn [31,32]. In addition, we have known that the addition of PEG1000 in the plating solution has an important role in the formation of the nanotree structure with many fine branches [1]. In the Cu electroplating solution, Cu metal ions are reduced at the cathodic Cu surface. Actually, composites of PEG-Cl-Cu are formed at the Cu surface, and they work as a diffusion barrier against the accumulation of Cu ions. Thus, the Cu deposition rate is significantly reduced by the addition of PEG

and Cl [33]. Therefore, it is speculated that PEG molecules adsorbed on specific CuSn crystal planes with high Miller indices suppress CuSn alloy deposition in our case. As a result, the anisotropic growth of CuSn nanowires along the $\langle 100 \rangle$ direction was enhanced by PEG addition. [1]

Figure 2 shows the results of nanotree oxidation. Figure 2(a) shows the nanotree before oxidation, and Fig. 2(b) shows the nanotree after thermal oxidation in air atmosphere at 350 °C for 30 min. After thermal oxidation, nanotree branches thickened owing to volume expansion by oxide formation. In addition, Fig. 3 shows the oxygen content of the nanotree evaluated by TEM-EDX. The oxygen content is about 20% at an oxidation temperature of 250 °C. It is shown that the oxygen concentration increases with increasing temperature. This causes a significant change in the morphology of nanotrees at temperatures higher than 350 °C.

Figure 4 shows the reflectance spectrum of the nanotree. The black spectrum corresponds to the nanotree before oxidation and the red spectrum corresponds to the nanotree after oxidation at 250 °C for 30 min in Fig. 4(a). We measured the reflectance spectra of pure copper [Fig. 4(b)] and pure tin [Fig. 4(c)] films as references. Both reflectances of pure copper and pure tin were high before oxidation, and a significant decrease was observed after oxidation.

Therefore, some amount of absorption occurred for a typical wavelength range for each case, reflecting the semiconducting property of the oxide. In the Cu oxide reflectance spectrum after oxidation [Fig. 4(b)], the reflectance decreased at wavelengths smaller than 850 nm, which well coincided with the band-edge absorption of CuO (E_g is about 1.2 eV) [34,35]. In addition, the reflectance decreased clearly at wavelengths smaller than 500 nm, which corresponded to the band edge absorption of Cu₂O (E_g is about 2.1 eV)

[36]. In the Sn oxide case [Fig. 4(c)], the reflectance decreased at wavelengths smaller than 400 nm, which coincided with the band-edge absorption of SnO₂ (E_g is 3.6 - 3.8 eV) [37].

In the case of the CuSn nanotree, the shape of the reflectance spectra differs from those of Cu and Sn oxides as well. The atomic composition of the CuSn nanotree is Cu : Sn = 81:19 [1]. Apparently, the spectrum shown in Fig. 4(a) cannot be obtained by simply adding those of Cu and Sn oxides. Both nanotree samples showed a very low reflectance in the visible wavelength range compared with that of usual metallic films. This may be due to the light trapping effect of the complex nanostructure. Otherwise, it is speculated that the low reflectance originates from the effect of a tapered structure such as a quadrangular prism in the GaSb nanotree [38]. After oxidation, the reflectance further decreases to 3 - 4%. There are several peaks in the reflectance spectra in the 200 - 350 nm wavelength range. The origin of these peaks has not been clarified yet; however, their behavior may suggest that the electronic band structure of the CuSn nanotree oxide is different from those of Cu and Sn oxides.

For the electrical measurement of the CuSn nanotree oxide, we formed a CuSn nanotree bridge on the split electrodes. We carried out CuSn electroplating until nanotrees grown on the Pt split gates connect with each other, and then measured the current–voltage characteristics of the CuSn nanotree oxide. Figure 5(a) shows a schematic drawing of Pt split electrodes with a gap of 10 μm formed by a lift-off technique on a SiO₂ substrate. Bridges of nanotrees were formed by CuSn electroplating on the split electrodes. It is shown that the nanotrees grown on the split gates are connected through the growth of CuSn nanotrees in Fig. 5(b). Figure 6 shows the temperature dependence of the conductivity of the CuSn nanotree oxide. The current–voltage characteristics of the

CuSn nanotree oxide bridge between Pt electrodes were linear, and we applied 1 V for resistance measurement. The results strongly suggest that the nanotrees are semiconductors because their conductance increases with increasing temperature.

Figure 7 shows the gas sensing property of the CuSn nanotree oxide formed by 250 °C annealing. Gases of H₂, O₂, CO, and N₂ were used as detection targets. We measured the change in conductance when gas is introduced into a chamber of the CuSn nanotree oxide. Gas was introduced after 50 s from the start of the measurement. The substrate temperature was 185 °C. The amount of each gas was 60 ml. The change in resistance started 30 s after the gas introduction. The result shows that the CuSn nanotree oxide conductance is sensitive against the introduction of H₂, O₂, and CO. After the gas was introduced, 30 s was needed for the change in resistance. It is considered that the delay is due to the transport of gas molecules from the inlet nozzle to the nanotree or the accumulation time of adsorbed molecules. The detailed mechanism is under investigation. When oxygen was adsorbed on the surface of the nanotree, the current increased, and when hydrogen or carbon monoxide was adsorbed, the current decreased. The CuSn nanotree oxide is a p-type semiconductor that shows an increase in conductivity caused by the adsorption of a negative charge, because O₂ molecules change to O⁻ ions after adsorption. However, the conductance decreases with the adsorption of a positive charge such as H⁺. The continuous change in conductance by H₂ adsorption may not only be related to the formation of the inversion layer but also to the diffusion of H atoms in the nanotree oxide [39,40]. When the gas supply is stopped, the resistance recovers to its initial value in most cases. When oxygen ions are adsorbed on the surface, an accumulation layer of holes is formed near the surface. The formation of the accumulation layer increases the conductivity. Thus, when oxygen was adsorbed on the surface of the

nanotree, the current increased. Furthermore, it is known that CuO_x is of the p-type, and SnO_x is of the n-type [34-37,41]. The present results strongly suggest that the nanotree oxide is a p-type semiconductor. There is some possibility of CuSnO_x formation, which has different electronic properties from CuO_x , and SnO_x .

4. Conclusions

We evaluated the photonic and electronic properties of CuSn nanotree oxides formed by annealing in atmosphere. After thermal oxidation, nanotree branches thickened owing to volume expansion by oxide formation. The reflectance of the CuSn nanotree oxide is as small as 6%, and it is further decreased to 3% by oxidation. Its spectrum is somehow different from those of CuO_x and SnO_x . The conductance of the CuSn nanotree oxide is sensitive against the adsorption of H_2 , O_2 , and CO gases. The CuSn nanotree oxide is a p-type semiconductor, because its conductivity increases with O^+ ion adsorption. The present results strongly suggest the possibility of the CuSn nanotree oxide as a gas sensor material with a high sensitivity. Further study regarding the oxidation temperature dependence of the properties of the nanotree oxide and its structure analysis will be necessary for the comprehensive understanding of the CuSn nanotree oxide.

Acknowledgement

This study was supported in part by the Strategic Project to Support the Formation of Research Bases at Private Universities, a Matching Fund Subsidy from the Ministry of Education, Culture, Sports, Science and Technology of Japan (MEXT).

References

- [1] T. Shimizu, Y. Tada, N. Kaneko, S. Tanaka, and S. Shingubara, *Surf. Coatings Technol.* **294**, 83 (2016).
- [2] A. Ponzoni, E. Comini, G. Sberveglieri, J. Zhou, S. Z. Deng, N. S. Xu, Y. Ding, and Z. L. Wang, *Appl. Phys. Lett.* **88**, 203101 (2006).
- [3] S. Park, S. Park, J. Jung, T. Hong, S. Lee, H. W. Kim, and C. Lee, *Ceram. Int.* **40**, 11051 (2014).
- [4] B. Wang, Z. Q. Zheng, L. F. Zhu, Y. H. Yang, and H. Y. Wu, *Sens. Actuators B* **195**, 549 (2014).
- [5] Z. Yin, Z. Wang, Y. Du, X. Qi, Y. Huang, C. Xue, and H. Zhang, *Adv. Mater.* **24**, 5374 (2012).
- [6] S. Sarkar and D. Basak, *Sens. Actuators B* **176**, 374 (2013).
- [7] M. A. Andio, P. N. Browning, P. A. Morris, and S. A. Akbar, *Sens. Actuators B* **165**, 13 (2012).
- [8] W. X. Jin, S. Y. Ma, A. M. Sun, J. Luo, L. Cheng, W. Q. Li, Z. Z. Tie, X. H. Jiang, and T. T. Wang, *Mater. Lett.* **143**, 283 (2015).
- [9] I. S. Hwang, J. K. Choi, S. J. Kim, K. Y. Dong, J. H. Kwon, B. K. Ju, and J. H. Lee, *Sens. Actuators B* **142**, 105 (2009).
- [10] S. Joshi, L. Satyanarayana, P. Manjula, M. V. Sunkara, and S. J. Ippolito, 2nd Int. Symp. Physics and Technology of Sensors (ISPTS), 2015, p.43.
- [11] A. Sharma, M. Tomar, and V. Gupta, *Sens. Actuators B* **181**, 735 (2013).
- [12] J. Y. Kwon, J. H. Ryu, Y. S. Jung, and S. M. Oh, *J. Alloys Compd.* **509**, 7595 (2011).

- [13] Q. Wan, Q. H. Li, Y. J. Chen, T. H. Wang, X. L. He, J. P. Li, and C. L. Lin, *Appl. Phys. Lett.* **84**, 3654 (2004).
- [14] Y. Wang, X. Jiang, and Y. Xia, *J. Am. Chem. Soc.* **125**, 16176 (2003).
- [15] A. Kolmakov, D. O. Klenov, Y. Lilach, S. Stemmer, and M. Moskovits, *Nano Lett.* **5**, 667 (2005).
- [16] L. Wang, Y. Kang, X. Liu, S. Zhang, W. Huang, and S. Wang, *Sens. Actuators B* **162**, 237 (2012).
- [17] T. Gao and T. H. Wang, *Appl. Phys. A* **80**, 1451 (2005).
- [18] Q. Wang, S. L. Qu, S. Y. Fu, W. J. Liu, J. J. Li, and C. Z. Gu, *J. Appl. Phys.* **102**, 103714 (2007).
- [19] E. R. Leite, I. T. Weber, E. Longo, and J. A. Varela, *Adv. Mater.* **12**, 965 (2000).
- [20] R. Ionescu, A. Hoel, C. G. Granqvist, E. Llobet, and P. Heszler, *Sens. Actuators B* **104**, 132 (2005).
- [21] W. J. Boettinger, C. E. Johnson, L. A. Bendersky, K. W. Moon, M. E. Williams, and G. R. Stafford, *Acta Mater.* **53**, 5033 (2005).
- [22] W. J. Choi, T. Y. Lee, K. N. Tu, N. Tamura, R. S. Celestre, A. A. MacDowell, Y. Y. Bong, and L. Nguyen, *Acta Mater.* **51**, 6253 (2003).
- [23] R. C. Pawar, J. S. Shaikh, S. S. Suryavanshi, and P. S. Patil, *Curr. Appl. Phys.* **12**, 778 (2012).
- [24] F. Zhu, H. Dong, Y. Wang, D. Wu, J. Li, J. Pan, Q. Li, X. Ai, J. Zhang, and D. Xu, *Phys. Chem. Chem. Phys.* **15**, 17798 (2013).
- [25] X. Sun, Q. Li, J. Jiang, and Y. Mao, *Nanoscale* **6**, 8769 (2014).

- [26] C. M. Lin, Y. C. Chang, J. Yao, C. Wang, C. Luo, and S. S. Yin, *Mater. Chem. Phys.* **135**, 723 (2012).
- [27] A. A. Firooz, A. R. Mahjoub, and A. A. Khodadadi, *Sens. Actuators B* **141**, 89 (2009).
- [28] F. Zhao, X. Li, J. G. Zheng, X. Yang, F. Zhao, K. S. Wong, J. Wang, W. Lin, M. Wu, and Q. Su, *Chem. Mater.* **20**, 1197 (2008).
- [29] M. J. Bierman, Y. K. A. Lau, A. V. Kvit, A. L. Schmitt, and S. Jin, *Science* **320**, 1060 (2008).
- [30] C. Cheng and H. J. Fan, *Nano Today* **7**, 327 (2012).
- [31] S. Shingubara, T. Shimizu, N. Kaneko, and Y. Tada, *Electrochem. Soc.* **15**, 1158 (2015).
- [32] B. Predel, *Landolt-Börnstein Group IV "Cu – Sn"* Springer, Heidelberg, (1994).
- [33] K. R. Hebert, S. Adhikari, and J. E. Houser, *J. Electrochem. Soc.* **152**, C324 (2005).
- [34] F. P. Koffyberg and F. A. Benko, *J. Appl. Phys.* **53**, 1173 (1982).
- [35] S. Anandan, X. Wen, and S. Yang, *Mater. Chem. Phys.* **93**, 35 (2005).
- [36] K. Mizuno, M. Izaki, K. Murase, T. Shinagawa, M. Chigane, M. Inaba, A. Tasaki, and Y. Awakura, *J. Electrochem. Soc.* **152**, C179 (2005).
- [37] J. Bandara, C. Divarathna, and S. Nanayakkara, *Sol. Energy Mater. Sol. Cells* **81**, 429 (2004).
- [38] C. Yan, X. Li, K. Zhou, A. Pan, P. Werner, S. L. Mensah, A. T. Vogel, and V. Schmidt, *Nano Lett.* **12**, 1799 (2012).
- [39] M. T. M. Koper and R. A. Van Santen, *Surf. Sci.* **422**, 118 (1999).

[40] K. Tsukada, T. Kiwa, T. Yamaguchi, S. Migitaka, Y. Goto, and K. Yokosawa, *Sens. Actuators B* **114**, 158 (2006).

[41] J. Tamaki, K. Shimanoe, Y. Yamada, Y. Yamamoto, N. Miura, and N. Yamazoe, *Sens. Actuators B* **49**, 121 (1998).

Figure captions

Fig. 1. (a) Cross-sectional SEM image and (b) top view of nanotrees grown for 60 min with cathode potential of -0.6 V. (d) Enlarged image of the nanotree branches indicated by the dashed box in (c).

Fig. 2. Cross-sectional SEM images of CuSn nanotree (a) before and (b) after oxidation at 300 °C for 30 min in atmosphere.

Fig. 3. Temperature dependence of oxygen concentration in CuSn nanotree oxide determined by EDX.

Fig. 4. (Color) Reflectance spectra of (a) CuSn nanotrees, (b) pure copper, and (c) pure tin before and after oxidation at 250 °C for 30 min.

Fig. 5. (Color) Schematic drawing of Pt split electrodes on SiO₂. (b) The split electrodes are connected by CuSn nanotrees.

Fig. 6. Temperature dependence of the conductivity of CuSn nanotree oxide.

Fig. 7. Change in current in the CuSn nanotree oxide device with introduction of various gases. Gas was introduced at t=50 s.

Figures

Fig. 1

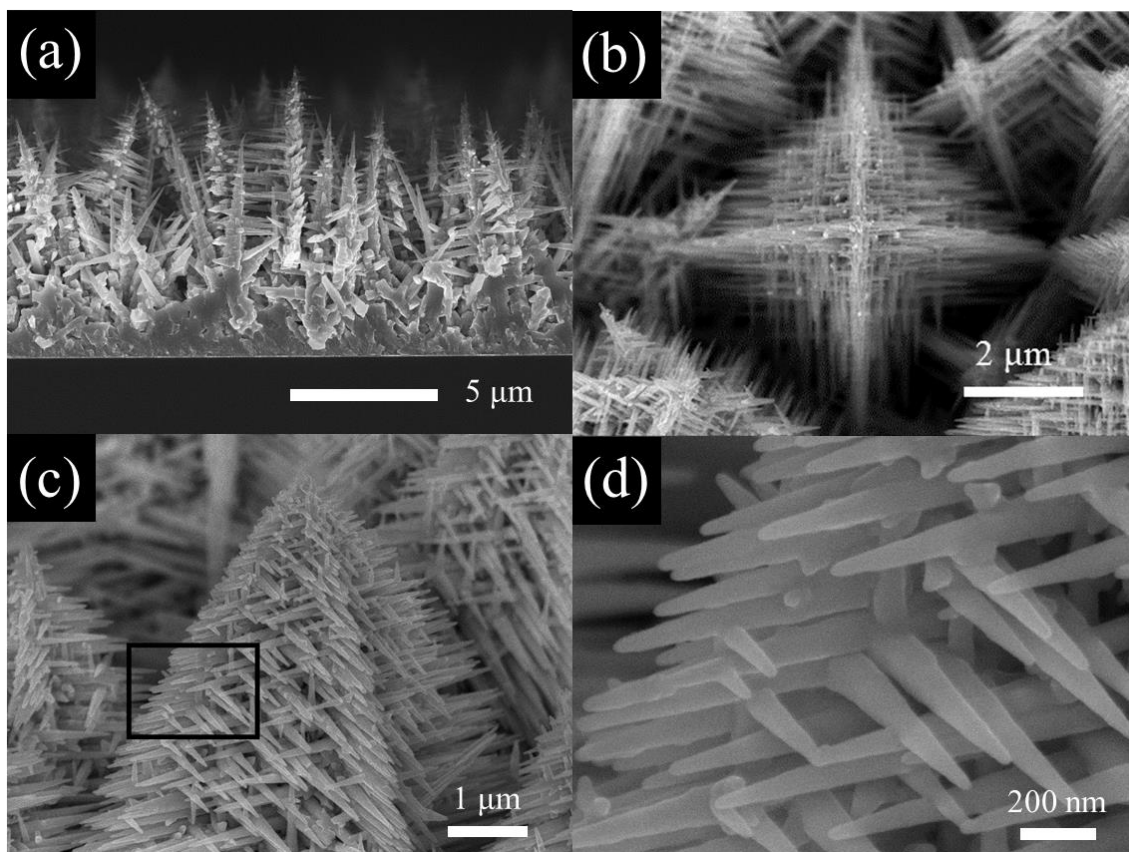


Fig. 2

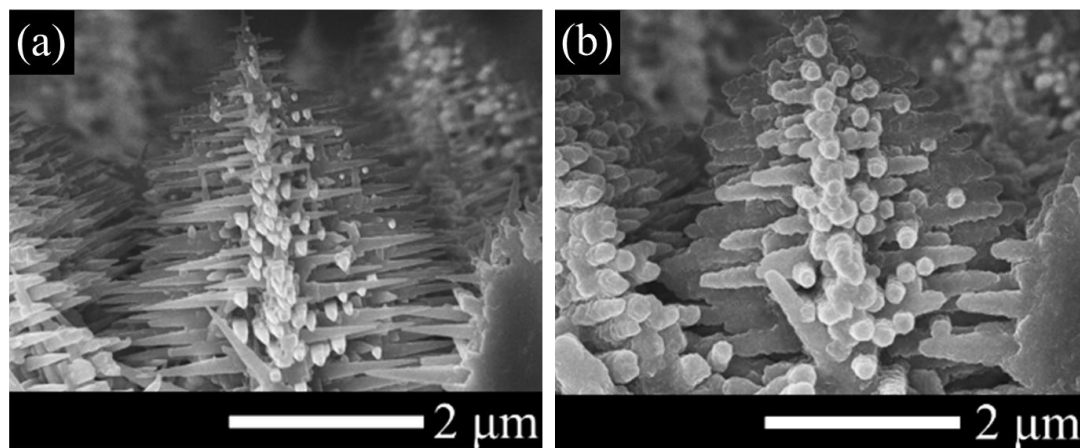


Fig. 3

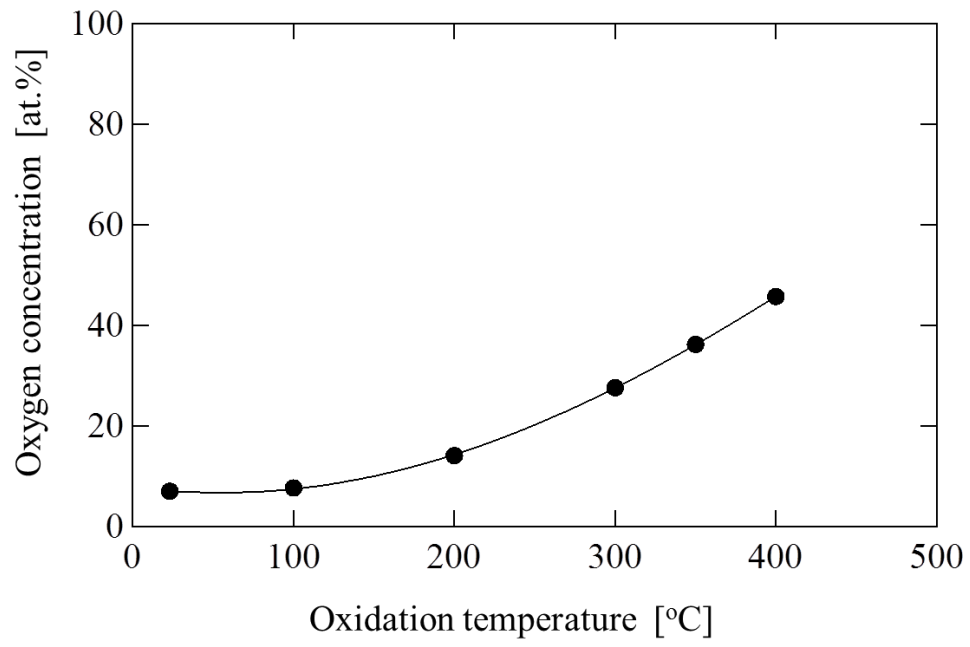
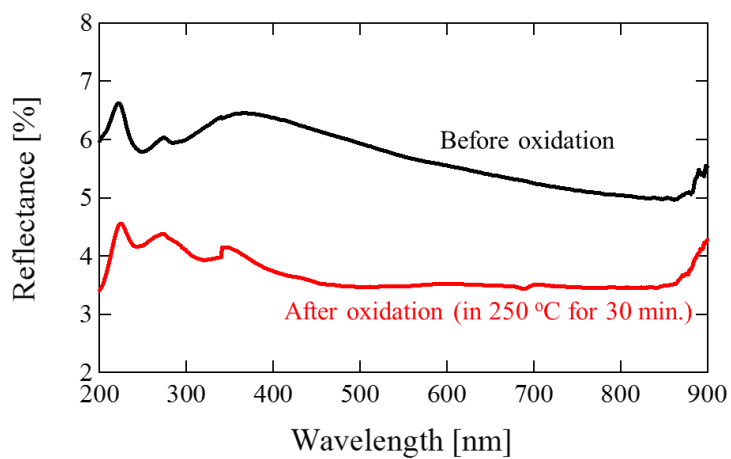
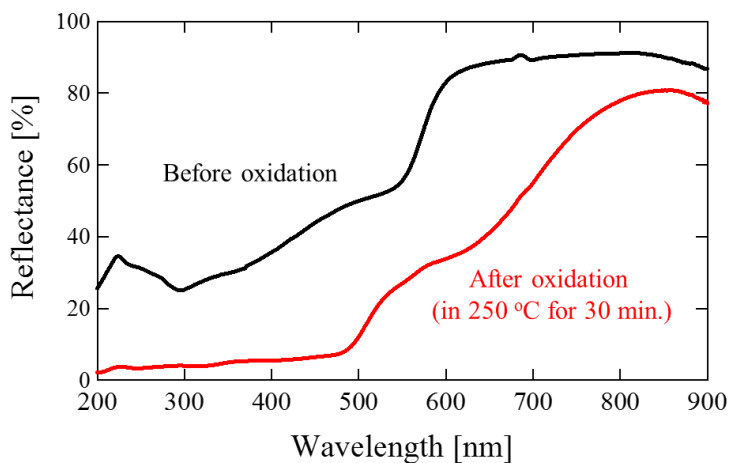


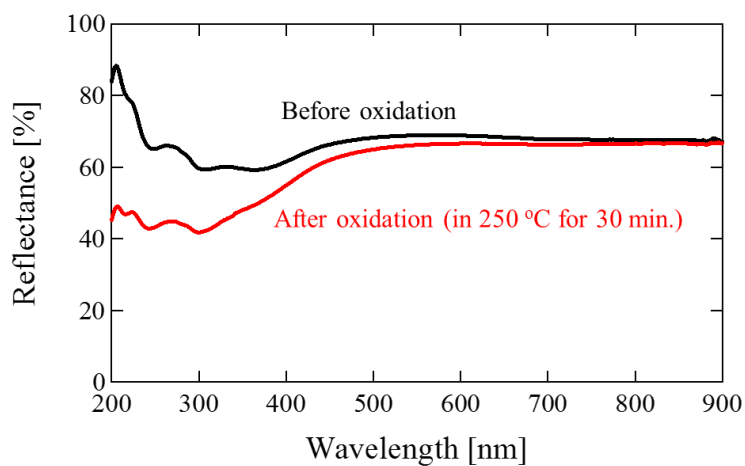
Fig. 4



(a)



(b)



(c)

Fig. 5

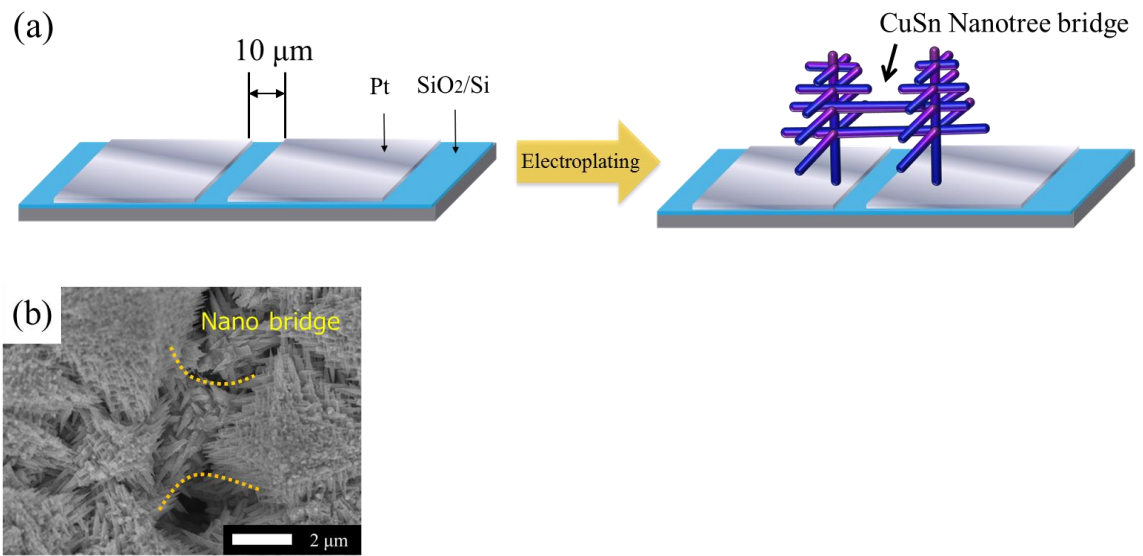


Fig. 6

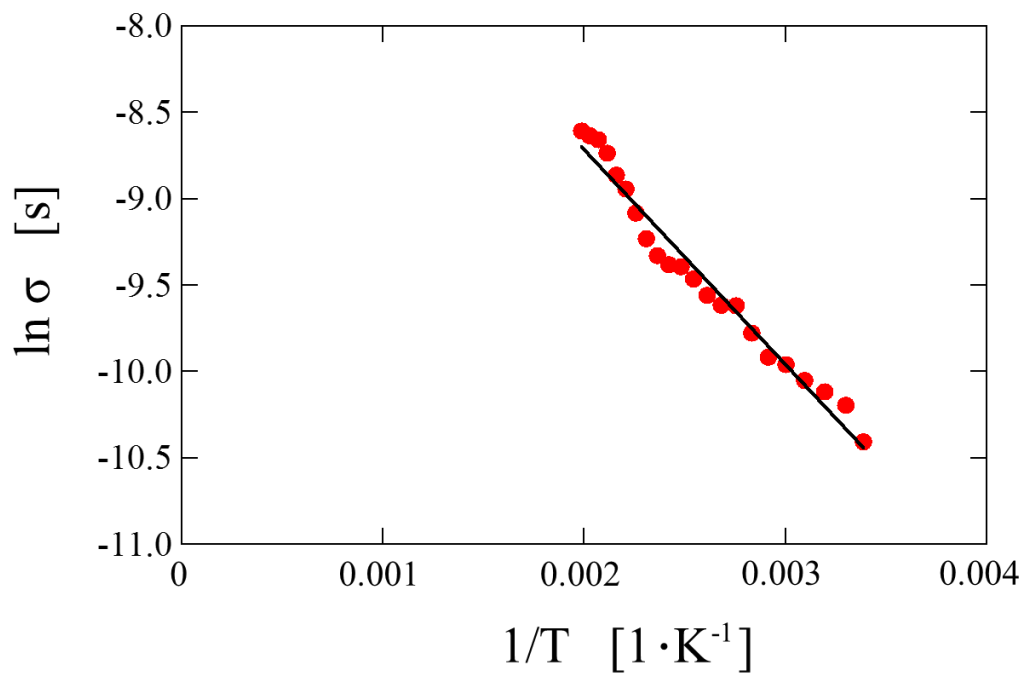


Fig. 7

